JOURNAL OF MATERIALS SCIENCE: MATERIALS IN MEDICINE **16** (2005) 119–128

Comparison between the *in vitro* surface transformations of AP40 and RKKP bioactive glasses

A. KRAJEWSKI[1], A. RAVAGLIOLI[1], A. TINTI[2], P. TADDEI[2,*], M. MAZZOCCHI[1], R. MARTINETTI[3], C. FAGNANO[2], M. FINI[4]
[1]*ISTEC-CNR, Via Granarolo 64, 48018 Faenza (Ravenna), Italy*
[2]*Dipartimento di Biochimica "G. Moruzzi", Sezione di Chimica e Propedeutica Biochimica, Via Belmeloro 8/2, University of Bologna, 40126 Bologna, Italy*
E-mail: paola.taddei@unibo.it
[3]*FinCeramica Faenza Srl., Faenza (Ravenna), Italy*
[4]*Servizio di Chirurgia Sperimentale, Ist. di Ric."Codivilla-Putti", IOR, Via di Barbiano 1/10, Bologna, Italy*

Two bioactive silica-phosphate glasses, AP40 and RKKP, were compared in their behaviour in simulated biological environment. Their chemical composition is practically identical, except that RKKP contains small amounts of amphoteric network-former oxides Ta_2O_5 and La_2O_3 (composition in wt% for AP40: β-$Ca_3(PO_4)_2$24.50, $SiO_2$44.30, CaO 18.60, Na_2O 4.60, K_2O 0.19, MgO 2.82, CaF_2 4.99; RKKP: β-$Ca_3(PO_4)_2$24.23, SiO_2 43.82, CaO 18.40, Na_2O 4.55, K_2O 0.19, MgO 2.79, CaF_2 4.94, Ta_2O_5 0.99, La_2O_3 0.09).

Previous investigations showed a better performance in osteopenic bone for RKKP. To gain more insight into these differences in biological behaviour, the *in vitro* bioactivity of the glasses was studied by treatment with a continuously replenished Hanks' Balanced Salt Solution (HBSS).

The glasses were examined before and after HBSS treatment for 20 and 40 days by X-ray Diffraction (XRD), Scanning Electron Microscopy (SEM), X-ray Energy Dispersion (EDX), Raman and IR vibrational spectroscopies.

Some slight but notable differences between the two glasses were observed after HBSS treatment. IR and EDX analyses showed that deposits formed on both glasses were composed of a calcium deficient carbonate-apatite; however, the layer formed on RKKP glass was found to be slightly more calcium deficient and thinner. EDX analysis evidenced the presence of a small percentage of F^- ions only in the layers formed on the RKKP samples.

The differences disclosed, although slight, can contribute to the understanding of the different biological behaviour previously observed.

1. Introduction

Bioactive materials have the property of forming a mechanically strong bond with living tissues (bone in particular) when implanted [1]. Due to these useful properties, the application of these materials in various areas of surgery is a subject of interest.

Bioactive glasses are specific materials which adapt themselves in a tissue environment and transform their surface by forming a calcium phosphate-rich layer when exposed to physiologic fluids [1, 2]. The first bioactive glass, in the system Na_2O-CaO-P_2O_5-SiO_2, was discovered in 1969 by Hench *et al.* [3]. Research in the last three decades has demonstrated that other ceramics also show a bone-bonding ability; this behaviour has suggested that the chemical composition of the glass may be modified to evoke its biological action [4–11], as supported by some previous experiences [12–14].

In this work two bioactive glasses, coded AP40 and RKKP, were studied. Their chemical composition is practically identical, except that RKKP contains small amounts of amphoteric network-former oxides Ta_2O_5 and La_2O_3.

In vitro investigations [15] have shown a greater cell growth around RKKP; as regards fibroblasts, those cultured on AP40 and RKKP plaques appeared flattened

*Author to whom all correspondence should be addressed.

TABLE I Chemical composition (wt%) of the AP40 and RKKP bioactive glasses tested in the present study and RKKP from reference [22]

Component	$\beta-Ca_3(PO_4)_2$	SiO_2	CaO	Na_2O	K_2O	MgO	CaF_2	Ta_2O_5	La_2O_3
AP40	24.50	44.30	18.60	4.60	0.19	2.82	4.99	–	–
RKKP	24.23	43.82	18.40	4.55	0.19	2.79	4.94	0.99	0.09
RKKP Ref. [22]	25.51	43.44	17.24	4.49	0.19	2.78	4.87	0.97	0.51

and exhibited long projections towards the porosity of the materials. Cell growth was greater for RKKP. Similarly, at light microscopy, osteoblasts evidenced better growth round RKKP. A semi-quantitative evaluation of cell growth round the two materials and on them was performed by SEM analysis: a nearly complete absence of osteoblasts was observed on AP40 and sparse clusters were revealed on RKKP. *In vivo* studies, in the already developed experimental surgery tests [15–17], have demonstrated the complete capability of both these glasses to bioattach to healthy bone, while only RKKP performs well in osteopenic bone [18].

Several studies have been carried out to clarify the reasons why the two glasses behave differently [9, 11, 19–22]. Recent investigations have been aimed at characterising the protein absorption profile onto AP40 and RKKP bioactive glass systems [21, 22], since several studies have suggested that the biocompatibility of an implant is to a large extent determined by selective absorption of protein from surrounding body fluids [23, 24]. Studies on the *in vitro* bioactivity and serum protein adsorption of zirconia coated by AP40 and RKKP glasses have shown a higher amount of total protein adsorbed on their surface than on zirconia alone [21]; the surface chemical characteristics of the two glass coatings substantially enhanced the integration of zirconia with bone cells at least *in vitro*, but no great differences between them were observed [21]. Other studies on bioactive glasses with similar compositions (the RKKP glass contained a markedly higher amount of La_2O_3 than ours, see Table I) [22] have evidenced that AP40 bound significantly more protein per surface unit than RKKP. However, the two glasses did not differ in protein absorption profiles: both have high affinity for apolipoprotein J, fibrinogen and fibronectin.

Previous studies [19] aimed at identifying some physico-chemical differences between the two glasses, have substantially failed. This new series of investigations was planned to reveal at least what differences in physico-chemical behaviour the two glasses exhibit when exposed to a continuously replenished saline solution simulating the body fluids.

The present work differs from previous ones [11, 20] since it was carried out on plates rather than granules or powders. Plates were used to have a wide plane area with a reproducibly polished surface similar to that used in previously reported *in vitro* and *in vivo* investigations [15, 18]. The use of plates rather than granules or powders assures that a significant amount of the underlying glass remains unaltered; in fact, only the sample surface (or in any case a thin layer) undergoes transformation. As regards powders, the smallest granules can undergo a complete transformation during ageing; in any case, their changes can be more significant than for bigger particles, so that the transformations can appear wider and less homogeneous [20].

2. Experimental

2.1. Materials

The composition of AP40 and RKKP is reported in Table I; the Ca/P atomic ratios are 3.0986 and 3.0992 for AP40 and RKKP respectively (with a mean of 3.0989 ± 0.0003).

Parallelepiped samples ($10 \times 10 \times 2$ mm) of AP40 and RKKP bioactive glasses were prepared [13]. The starting powders (with weight ratios according to Table I) were melted in a Pt crucible in a laboratory kiln at 1450 °C for 60′ and poured into a graphite die. After cooling to room temperature, the samples were polished with a series of diamond-papers up to 1 μm grain size.

For the *in vitro* tests, according to other authors [25–27], the commercially available (Sigma ref. H8264) Hanks' Balanced Salt Solution at pH 7.3 (HBSS) was utilised to simulate the body fluids; its chemical composition is reported in Table II.

2.2. Methods

In order to study the *in vitro* bioactivity, each sample was separately placed in a special device at 37 °C for 2 set times (20 and 40 days): the sample was completely immersed in HBSS under a continuous re-circulation of this solution through a pipe and a small pump. The flux of the liquid was 1 mm^3 sec^{-1}. The use of this type of device does not allow the formation of ionic concentration gradients around the sample, so that what happens in an *in vivo* implant is simulated in a more realistic way. At each set time, the samples were recovered from the solution, gently rinsed with a little distilled water and put in an oven at 40 °C until dry.

The surface of the samples was characterised by X-ray Diffraction (XRD), Raman and Infrared (IR) vibrational spectroscopies, Scanning Electron Microscopy (SEM) and micro-chemical analysis by X-ray energy dispersion (EDX) microprobe. In addition, the roughness was tested on the polished surfaces of the untreated samples.

XRD investigation was carried out by a Rigaku Miniflex (Cu K_α) device, with 2.5 °/min 2θ step size.

IR spectra were recorded with a Fourier Transform FT-IR Jasco 300 E Model spectrometer with spectral

TABLE II Ionic composition of HBSS

Ion	Na^+	K^+	Ca^{2+}	Mg^{2+}	HCO_3^-	Cl^-	HPO_4^{2-}	SO_4^{2-}
Amount (mM)	141.5	5.8	1.3	0.8	4.2	144.9	0.8	0.8

resolution of 4 cm^{-1}. The spectra were obtained on KBr pellets (about 0.5% w/w) containing finely ground powder of the glasses, in the case of the untreated samples, and their gently removed surfaces, for the samples treated with HBSS. The carbonate content was spectroscopically evaluated according to the procedure described by Featherstone *et al.* [28]; these authors reported that the ratio of the extinction of the IR carbonate band at about 1425 cm^{-1} to the extinction of the IR phosphate band at about 565 cm^{-1} (E_{1425}/E_{565}) is linearly related to the carbonate content of the carbonate-apatite. The E_{1425}/E_{565} was determined from the recorded spectra; the corresponding carbonate content was calculated by interpolation from the calibration line obtained by plotting the E_{1425}/E_{565} ratio against the carbonate content for a series of mixtures (2, 5, 10 and 15% wt/wt) of $BaCO_3$ and hydroxyapatite (Aldrich-Chemie GmbH & Co, Steinheim, Germany). The experimental equation ($R = 0.998$) utilised for calculating the carbonate content was:

$$[\%\ CO_3] = 17.1\,[E_{1425}/E_{565}]$$

The method allows carbonate estimation to better than $\pm 10\%$ in the range 1–12% wt/wt [28].

Raman spectra were recorded on untreated and treated massive glasses by using a Bruker IFS66 spectrometer, equipped with a FRA-106 FT-Raman module and a N_2 liquid cooled Ge-diode detector. The excitation source was a Nd^{3+}-YAG laser (1064 nm) in the backscattering configuration. The focused laser beam was $\sim$100 μm, spectral resolution 4 cm^{-1} and laser power at the sample $\sim$180 mW.

SEM investigations were performed by a Cambridge 5360, equipped with analytical microprobe (EDX; Link Exl II). The samples submitted to SEM investigations were covered with a thin carbon film sputtered by physical vapour deposition (PVD). They were examined through secondary electrons and backscattered electron imaging (open window, Energy $<$10 keV) to check all possible light elements on different points (on small areas of about 50 μm^2) with (apparently) different micromorphology. As the composition appeared practically identical on all different points and on all different samples, we decided to perform a more accurate quantitative analysis on a wide area (about 10^4 μm^2) on every sample to detect the Ca/P atomic ratio on the surface. This quantitative analysis was carried out under 15 keV, with Be window inserted, and gain calibration on Ti. ZAF correction procedure was applied.

3. Results

3.1. X-ray diffraction

XRD revealed the formation of an apatite layer on the samples treated with HBSS. The crystallinity detected by this technique varied from sample to sample. XRD data are summarised in Table III [29].

At increasing immersion times in HBSS, small 2θ co-ordinate shifts of the peaks were noticed: towards higher d_{hkl} values for AP40 samples, in the opposite direction for RKKP. With reference to the most central and notable peaks (those corresponding to the list numbers from 10 to 12 of Table III), interesting trends were observed. The diffraction patterns recorded on the surface of the RKKP samples maintain their main peak at about 2.81 Å, which coincides with that of the JCPDS card of hydroxyapatite (HA); instead, in the spectra recorded on the surface of the AP40 samples, the main peak appears at 2.775 Å (after 20 days of treatment in HBSS) and 2.709 Å (after 40 days).

As concerns XRD patterns of the AP40 samples treated for 20 days, the peak intensities were distributed in a different way with respect to the JCPDS card of HA. In particular, the peaks which strongly involve the *c*-axis of HA exhibited lower intensities if compared with the other diffraction peaks; this behaviour can be interpreted as a preferential orientation with the *c*-axis parallel to the surface [30]. However, the AP40 samples immersed in HBSS for 40 days produced X-ray patterns with peaks that reorganised to a closer correspondence with those of HA.

3.2. IR investigations

Figs. 1 and 2 report the IR spectra corresponding to AP40 and RKKP before and after treatment in HBSS for 20 and 40 days. Table IV reports the observed bands with their assignments in comparison with those of HA (from references 31 and 32). The IR spectra of untreated AP40 and RKKP glasses (Figs. 1(a) and 2(a)) are very similar and show broad absorptions at about 1030–1040 cm^{-1} (ν SiO^-), 955 cm^{-1} (ν_{as} SiOSi), 770 cm^{-1} (ν_s SiOSi) and 490 cm^{-1} (δ SiOSi and δ OSiO), all attributable to a silicate glass component (Table IV) [1, 33, 34]. Both the untreated glasses show the presence of narrow bands, overlapping the above reported ones, at about 1090 cm^{-1} (ν_3 PO_4 stretching), 1055 cm^{-1} (ν_3 PO_4 stretching, shoulder), 1040 cm^{-1} (ν_3 PO_4 stretching), 605 cm^{-1} (ν_4 PO_4 bending), 575 cm^{-1} (ν_4 PO_4 bending, shoulder) and 565 cm^{-1} (ν_4 PO_4 bending) all attributable to a crystalline calcium phosphate component (Table IV) [31, 32, 35]. Also Salinas *et al.* [36], who studied CaO-SiO_2-P_2O_5 sol-gel glasses, observed the presence of a doublet at 565–597 cm^{-1}, characteristic of a crystalline phosphate; according to these authors, this doublet is ascribable to the presence of phosphate nuclei formed in the glassy structure during synthesis.

In order to evaluate the crystallinity degree of both untreated glasses, the 1040 cm^{-1} bandwidth was calculated at its half height in the normalised spectra of Figs. 1(a) and 2(a). This bandwidth was about 222 and 213 cm^{-1} for the AP40 and RKKP untreated glasses respectively (Table V); this finding suggests a more ordered structure for the RKKP glass.

It is interesting to notice that the layers formed on the surface of these glasses, after immersion in HBSS, do not produce any signal attributable to silicate groups (Figs. 1(b), (c), and 2(b), (c)). Consequently silicates appear to be absent altogether in the formed layers and this result agrees with XRD and EDX findings (see below). The spectra of both the series are very similar: they show the bands typical of a crystalline calcium

TABLE III The most notable d_{hkl} values (Å) and their corresponding relative intensities (I/I_0) obtained from X-ray diffraction of AP40 and RKKP; the d_{hkl} (Å) and I/I_0 values from the JCPDS card of hydroxyapatite are reported for comparison

Sample	**AP40**				**RKKP**				**HA**	
time (days)	20		40		20		40			
X-ray quality: N/S%[1]	Highly crystalline 2.5		Sufficiently crystalline 6.0		Almost amorphous 16		Sufficiently crystalline 7.5		JCPDS card n. 9-432	
Peak n.	d_{hkl}	I/I_0	d_{hkl}	I/I_0	d_{hkl}	I/I_0	d_{hkl}	I/I_0	d_{hkl}	I/I_0
1	7.494	3	8.021	7			8.170	5	8.170	12
2	6.013	6	5.262	12	5.998	10	5.302	6	5.260	6
3	4.98	8					4.725	5	4.720	4
4	4.045	4	4.165	15			4.070	10	4.070	10
5							3.880	10	3.880	10
6									3.510	2
7	3.440	30	3.445	47	3.440	48	3.430	50	3.440	40
8	3.173	5	3.174	15			3.176	5	3.170	12
9	3.072	15	3.068	20	3.048	18	3.064	80	3.080	18
10	2.801	47	2.802	94	2.815	100	2.804	100	2.814	100
11	2.775	100	2.781	60	2.790	40	2.774	40	2.778	50
12	2.703	16	2.709	100	2.719	60	2.706	60	2.720	60
13	2.623	7	2.629	30			2.629	7	2.631	25
14	2.467	3	2.250	4	2.250	10			2.528	6
15			2.280	2			2.296	40	2.296	8
16	2.252	22	2.256	43			2.253	20	2.262	20
17									2.223	2
18									2.209	1
19	2.142	5			2.146	12	2.142	5	2.143	10
20							2.134	4	2.134	4
21									2.065	8
22	2.030	3	2.030	5	2.034	8			2.040	2
23									2.000	6
24	1.938	10	1.940	30	1.939	30	1.936	28	1.943	30
25	1.884	8	1.889	7			1.913	12	1.890	16
26			1.860	16			1.884	20	1.871	6
27	1.839	16	1.841	36	1.851	41	1.838	35	1.841	40

[1](N/S)% = noise on signal ratio percent; it corresponds to the percent probable error of net in the acquisition by the detector of all photons which correspond to those coming from the specific reflection and those coming from the background [29]. The higher the value, the lower the degree of cristallinity.

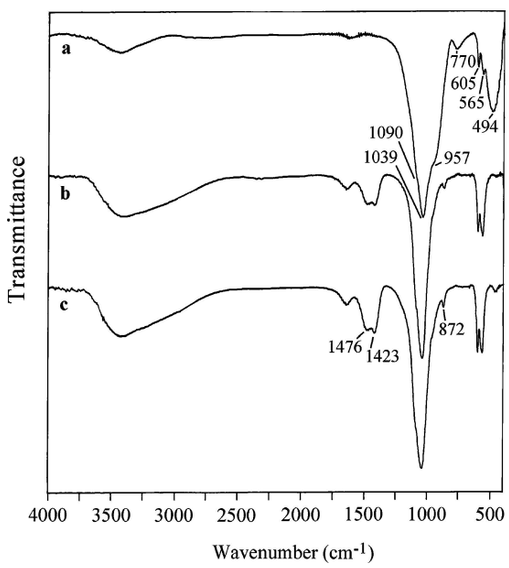

Figure 1 IR spectra corresponding to the AP40 glass at different times of treatment with HBSS: (a) $t = 0$, (b) $t = 20$ days, and (c) $t = 40$ days.

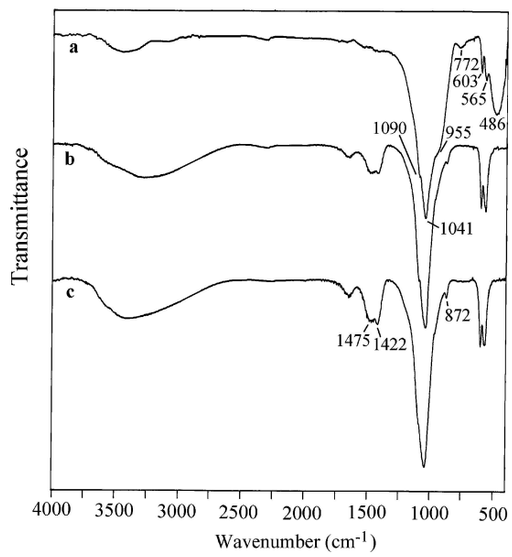

Figure 2 IR spectra corresponding to the RKKP glass at different times of treatment with HBSS: (a) $t = 0$, (b) $t = 20$ days, and (c) $t = 40$ days.

TABLE IV Wavenumbers, assignments and relative intensities (referred to the 1040 cm^{-1} band) of the IR bands observed in the 1500–400 cm^{-1} range for AP40 and RKKP glasses before and after treatment in HBSS. The data corresponding to hydroxyapatite (HA) [31, 32] are reported for comparison

Assignments (silicate glasses) [1, 33, 34]	AP40 $t=0$	RKKP $t=0$	AP40 $t=20$ days	AP40 $t=40$ days	RKKP $t=20$ days	RKKP $t=40$ days	HA [31, 32]	Assignments (carbonato-apatites) [31, 32, 35, 37]
			1480 (14)	1476 (18)	1477 (12)	1475 (17)		ν CO_3 stretching B-type carbonato-apatite
			1425 (14)	1423 (19)	1425 (13)	1422 (18)		ν CO_3 stretching B-type carbonato-apatite
				1190 (10) sh	1190 (12) sh	1200 (11) sh		ν_5 POH bending HPO_4^{2-} ion
	1090 (77) sh	1090 (74) sh	1090 (69) sh	1090 (71) sh	1091 (69) sh	1091 (69) sh	1088	ν_3 PO_4 stretching
	1055 (96) sh	1050 (96) sh	1051 (98) sh	1055 (97) sh	1055 (95) sh	1055 (95) sh	1065	ν_3 PO_4 stretching
	1039 (100)	1041 (100)	1040 (100)	1040 (100)	1040 (100)	1041 (100)	1035	ν_3 PO_4 stretching
ν SiO^-	~1030–1040 br	~1030–1040 br						
ν_{as} SiOSi	957 (68) sh	955 (60) sh	960 (19) sh	964 (21) sh	960 (24) sh	965 (22) sh	962	ν_1 PO_4 stretching
			869 (7)	872 (9)	874 (8)	872 (7)		δ CO_3 B-type carbonato-apatite
ν_s SiOSi	770 (8)	772 (6)						
							630	δ OH
	605 (17)	603 (17)	605 (27)	604 (28)	604 (29)	603 (28)	602	ν_4 PO_4 bending
	575 (17) sh	575 (19) sh	577 (26) sh	575 (27) sh	575 (28) sh	575 (27) sh	574	ν_4 PO_4 bending
	565 (20)	567 (21)	568 (29)	567 (29)	566 (31)	568 (27)	565	ν_4 PO_4 bending
δ SiOSi and δ OSiO	494 (40)	486 (39)						

ν_s = symmetric stretching; ν_{as} = asymmetric stretching; δ = bending; br = broad; sh = shoulder.

TABLE V Width of the bands at 1040 cm^{-1} (IR) and 963 cm^{-1} (Raman) at their half height calculated from the normalised spectra reported in the Figures numbered from 1 to 4. Carbonate contents (wt%) calculated from the IR spectra according to the procedure described by Featherstone *et al*. [28]

	AP40			RKKP		
	$t=0$	$t=20$ days	$t=40$ days	$t=0$	$t=20$ days	$t=40$ days
Width of the IR band at 1040 cm^{-1} at its half height (cm^{-1})	222	112	111	213	114	112
Carbonate content (wt%)	–	8	10	–	7	11
Width of the Raman band at 963 cm^{-1} at its half height (cm^{-1})	26	18	16	16	14	13

phosphate (Table IV) [31, 32, 35]. The crystallinity of the layers formed on the glasses is confirmed by the decrease of the 1040 cm^{-1} bandwidth with respect to the corresponding untreated glasses (Table V). As regards the crystallinity of the deposits, no significant differences between the two glasses were observed at increasing immersion time in HBSS (Table V).

The spectra of Figs. 1(b), (c), and 2(b), (c) do not exhibit any trace of the bands at 3570 cm^{-1} (ν OH stretching) and 630 cm^{-1} (δ OH bending) typical of HA [31, 32] (Table IV). Moreover, these spectra show bands at about 1480, 1425 and 870 cm^{-1} typical of a B-type carbonate-apatite [37, 38] (Table IV), i.e., an apatite compound in which CO_3^{2-} substitutes PO_4^{3-} rather than OH^- (A-type carbonate-apatite). As can be seen from Table V, the carbonate content increases for both glasses passing from 20 to 40 days of treatment in HBSS, reaching, at the end, a value of about 10 wt%. No significant differences in the trend of the carbonate content were observed for the two glasses, the associated error being about ± 1 wt%.

The only difference observed in the spectra of the layers formed on the two glasses consists of the presence of a weak broadening at about 1190 cm^{-1}, attributable to HPO_4^{2-} ions (ν_5 POH bending) [35], more evident in the layers formed on RKKP samples (Figs. 2(b) and (c)).

3.3. Raman investigations

Figs. 3 and 4 report the Raman spectra corresponding to AP40 and RKKP samples respectively before and after treatment in HBSS for 20 and 40 days. The spectrum of the RKKP untreated glass (Fig. 4(a)) shows the bands at 1075 cm^{-1} (ν_3 PO_4 stretching), 1054 cm^1 (ν_3 PO_4 stretching), 1040 cm^{-1} (ν_3 PO_4 stretching), 963 cm^{-1} (ν_1 PO_4 stretching), 606 cm^1 (ν_4 PO_4 bending), 592 cm^{-1} (ν_4 PO_4 bending), 583 cm^{-1} (ν_4 PO_4 bending), 444 cm^{-1} (ν_2 PO_4 bending), and 430 cm^{-1} (ν_2 PO_4 bending), typical of a crystalline calcium phosphate [31, 32, 35]. These bands overlap the broad bands at about 1050 cm^1 (ν SiO^-, disilicate), 930 cm^1 (ν SiO^-, metasilicate) and 600 cm^1 (ν_s SiOSi, metasilicate) typical of silicate glasses [39–43]. The spectrum of the AP40 untreated sample (Fig. 3(a)) shows a similar trend but the bands due to the phosphate group are less evident, confirming the higher amorphous character of this glass, as revealed by the IR results. This finding is also confirmed by the 963 cm^{-1} bandwidth (Table V) which was 26 and 16 cm^{-1} for the AP40 and RKKP untreated glasses respectively.

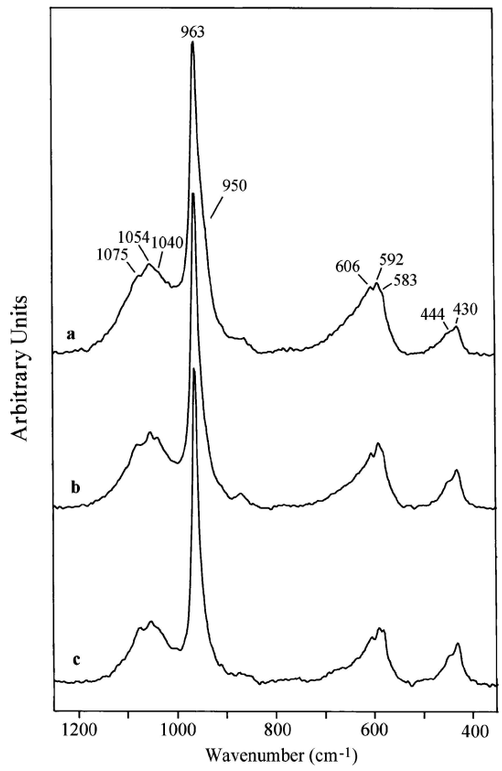

Figure 3 Raman spectra of the AP40 glass at different times of treatment with HBSS: (a) $t = 0$, (b) $t = 20$ days, and (c) $t = 40$ days.

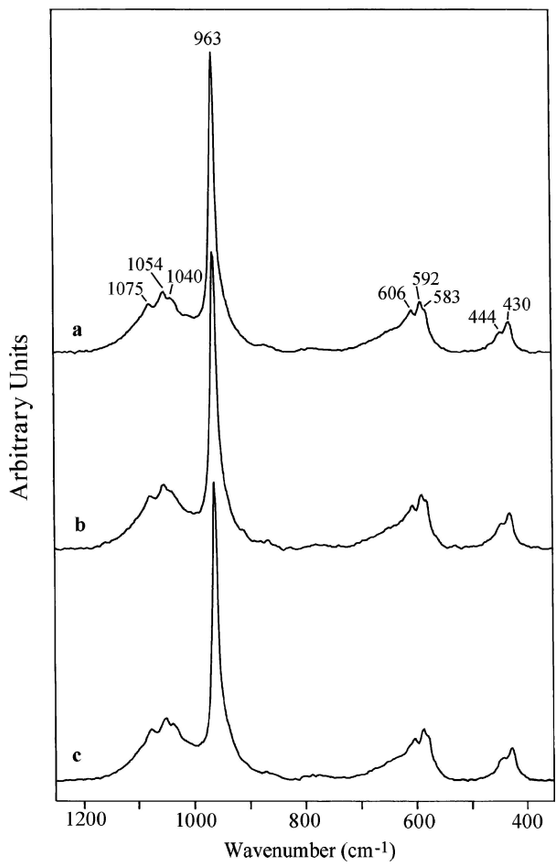

Figure 4 Raman spectra of the RKKP glass at different times of treatment with HBSS: (a) $t = 0$, (b) $t = 20$ days, and (c) $t = 40$ days.

As regards the spectra of Figs. 3(b), (c), and 4(b), (c), it has to be recalled that they were recorded on the massive glasses; therefore, they reflect the composition of both the surface and the underlying glass.

The Raman results appear more interesting for the AP40 glass: at increasing immersion times in HBSS, the 963 cm^{-1} bandwidth decreases (Table V) and the bands attributed to PO_4^{3-} ions appear more resolved. This finding can be explained according to the IR results; since no increase in crystallinity was revealed by IR investigations passing from 20 to 40 days of treatment in HBSS, the decrease of the 963 cm^{-1} bandwidth reveals that the contribution given by the surface layer to the Raman signal progressively increases. Therefore, a progressive increase of the thickness of the layer formed on the glass occurs. A similar behaviour is hardly detectable for the RKKP sample because of its greater starting molecular order.

3.4. SEM and EDX investigations

Figs. 5 and 6 show the SEM microphotographs of the AP40 and RKKP samples respectively, treated with HBSS for 20 (a) and 40 days (b). The surface of both glasses appears substantially homogeneously smooth after 20 days of treatment in HBSS (Figs. 5(a) and 6(a)); this could indicate that, at this stage, calcium phosphate deposition occurs by superimposition of growing layers. On the contrary, the surface of the samples treated in HBSS for 40 days (Figs. 5(b) and 6(b)) shows many aggregates of micro-spheroidal particulate, whose formation could be related to local rearrangements. Qualitative investigations, by EDX microprobe (10 keV, without Be window, carried out in the points indicated in the Figs. 5 and 6), have demonstrated the presence of detectable amounts of Na^+ and Mg^{2+} on all the samples. A small amount of F^- was detected only on the RKKP samples (its amount was estimated to be about 0.5 at.%). Silicon was observed only in point A of Fig. 6(a). This finding could be attributed to the very thin surface layer formed on RKKP after 20 days of treatment; therefore, the electron beam excited a small portion of the underlying glass.

Quantitative analysis carried out by EDX microprobe (15 KeV, Be window inserted) gave the results reported in Table VI. The excitation of elements present in the underlying glass by the electronic beam becomes progressively less probable with the time of HBSS treatment and consequently the corresponding signal decreases as the formed layer becomes progressively

TABLE VI Microanalytical data obtained by EDX investigation of the cited samples (± 6%)

Sample	AP40		RKKP	
Time in HBSS (days)	20	40	20	40
Element	Atom%	Atom%	Atom%	Atom%
Ca	20.8	21.2	20.7	21.2
P	15.1	15.7	15.7	15.8
Na	0.59	0.78	1.01	0.83
Mg	0.84	0.42	0.85	0.61
Si	1.13	0.32	0.25	0.076
Ca/P ratio	1.39	1.35	1.32	1.34

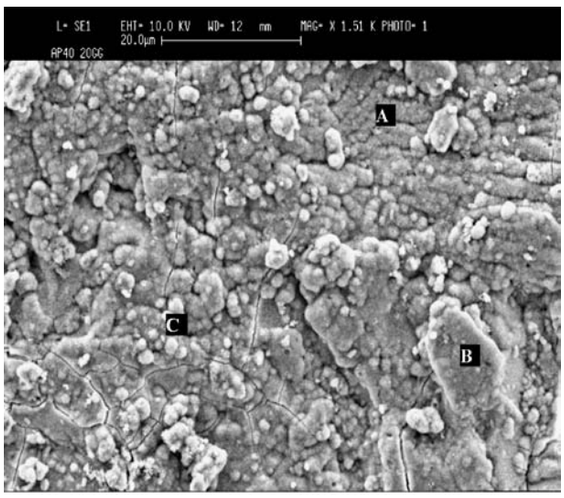

(a)

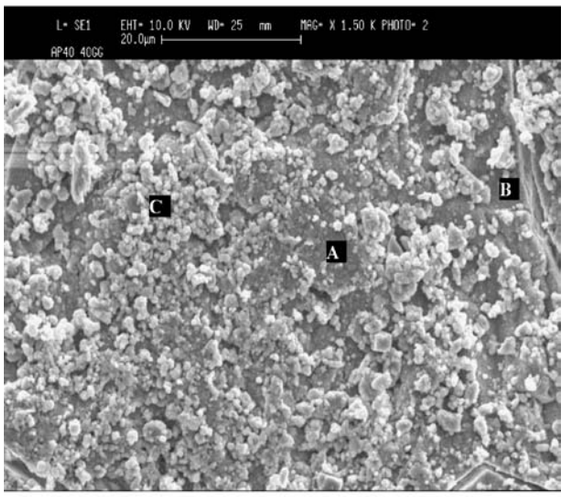

(b)

Figure 5 View of the surface of an AP40 sample after 20 (a) and 40 days (b) of HBSS treatment; the points where local qualitative analysis was carried out are indicated.

thicker. The results reported in Table VI on silicon suggest that, at a given immersion time in HBSS, the layer formed on the AP40 samples should be thicker than on RKKP, according to the Raman results.

3.5. Micromorphological investigations

SEM observations on cross-sectioned samples demonstrated that the apatite layers formed tended to fill all the cavities present on the glass surface and form a more regular external surface. Table VII reports the thickness of the layers formed on AP40 and RKKP samples treated with HBSS for 20 and 40 days.

TABLE VII Thickness of the layers formed on AP40 and RKKP treated with HBSS for 20 and 40 days

Days	Layer thickness (μm)	Mean layer thickness (μm)
AP40 20	15–25	20
AP40 40	25–50	40
RKKP 20	5–25	15
RKKP 40	20–50	30

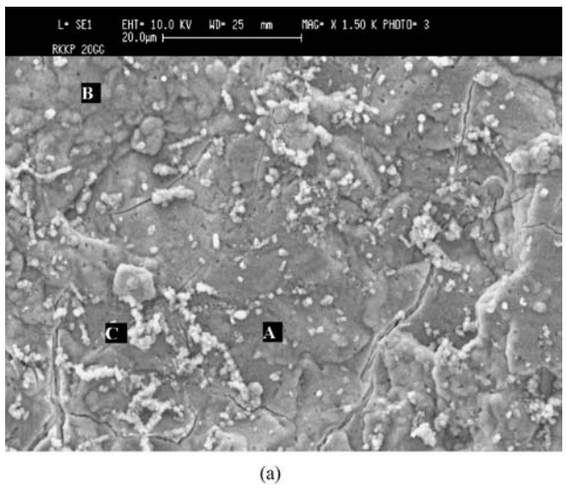

(a)

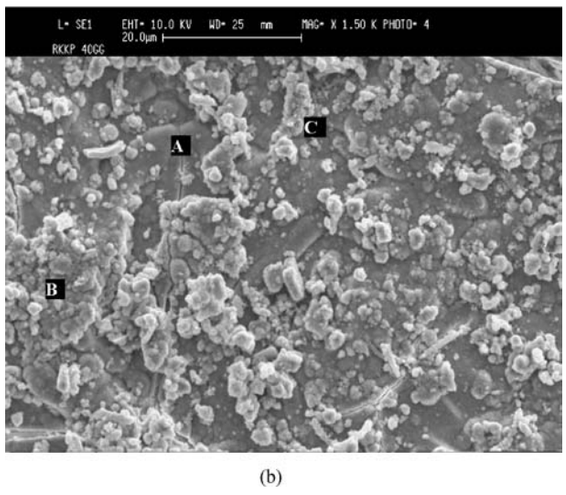

(b)

Figure 6 View of the surface of an RKKP sample after 20 (a) and 40 days (b) of HBSS treatment; the points where local qualitative analysis was carried out are indicated.

From these data it results that a mean thicker layer formed on AP40 samples. At increasing immersion times, the thickness of the layer increased (from about 20 μm after 20 days of treatment in HBSS to about double after 40 days), confirming the Raman results and the increasing masking of the Si detection in EDX measurements (Table VI).

On the surface of the AP40 samples treated for 20 days in HBSS, needle-shaped micro-crystals (composed of calcium phosphates, as revealed by EDX and vibrational spectroscopy) were observed. On the other hand, they were not observed on the RKKP samples treated in the same way. These morphological differences may reflect the compositional differences revealed by XRD spectra.

After 40 days of treatment, micro-spherulitic shapes tend to be present on the surface of both glasses; they are attributable to calcium phosphates, as revealed by XRD, EDX and vibrational spectroscopy.

4. Discussion

Many techniques (XRD, IR and Raman spectroscopies, SEM, TEM, energy dispersive spectroscopy EDS, electron diffraction ED) have been extensively used to study

surface reactions on bioactive glasses after treatment with simulating body fluids [30, 44–56]. A common behaviour observed for bioactive glasses, independently of their specific composition, is the formation of a calcium phosphate-rich layer on their surface upon soaking with simulating body fluids. Many authors have reported that amorphous calcium phosphates, initially formed, crystallise to hydroxycarbonate-apatites and carbonate-apatites analogous to those present in bone [30, 44–56].

This work was aimed at identifying the differences between the *in vitro* surface reactivity of AP40 and RKKP glasses in order to give a possible explanation of their different biological behaviour.

The samples were analysed after 20 and 40 days of *in vitro* ageing on the basis of the results of the *in vivo* clinical evaluations; histomorphometric analyses have shown that at 20 days (unpublished results) osteointegration was in progress, while at 40 days the material-bone bonding was the same as after 56 days [57]. The latter experimental time had revealed to be characterised by the most important differences which were evident until 24 weeks; after this time, the material-bone bonding would have been completed and further intensive remodelling of bone would not occur. On the other hand, several studies reported in the literature have analysed glass behaviour after few hours or days of ageing [36, 44–46, 48, 52–56]. The present study was prevalently focused on the "long-term" ageing of the AP40 and RKKP glasses, rather than on the beginning of calcium phosphate deposition. However, previous studies on granules aged for 2 days showed the deposition of a calcium phosphate with a Ca/P molar ratio of about 1, even if this value was probably strongly affected by the underlying glass. Actually, this can be related to the fact that the glasses tested in the present study underwent surface transformations slower than the Hench bioglass.

SEM analysis indicated that the surface of both the glasses progressively underwent morphology changes upon immersion in HBSS. Both AP40 and RKKP appear substantially homogeneously smooth after 20 days in HBSS, while an enrichment in granular spheroidal aggregates was visible after 40 days. The formation rate of the apatitic layer and its crystallinity may depend on a number of different physical properties of the glass surface. Among all possible parameters, two in particular have been taken into account in the recent literature: roughness [30], which has been shown to influence also cell attachment [58] and the presence of original nano-crystals whose amount proportionally decreases the formation rate of carbonate-apatites [48]. At this purpose, both the untreated glasses were found to have a substantially equal roughness, as detected by microscopy. On the contrary, the crystallinity of the two glasses was notably different. In agreement with results reported by Filho *et al.* [48], we observed a lower reactivity (i.e., a mean lower thickness of the deposit) for the more crystalline glass, i.e., RKKP.

IR spectroscopy indicated that the deposits formed on both glasses were constituted of B-type carbonate-apatites. Micro-chemical EDX investigations demonstrated that these apatites were calcium deficient, as shown by the Ca/P molar ratios reported in Table VI. In the light of the XRD results, we tried to identify the deposits formed on AP40 and RKKP glasses. The small shifts observed in the XRD peaks and the trend of the I/I_0 values were consistent with the small variations in composition observed by micro-chemical EDX. This investigation excluded any significant presence of silicon in the formed layers; therefore all compounds that contained it had to be discarded. Micro-analytical analysis of the deposited layers (Table VI) revealed a very low content of cations that might substitute Ca^{2+}, such as Na^+ and Mg^{2+}; consequently they scarcely contributed to the observed calcium deficiency of the apatitic layers formed. Because sodium and magnesium were present to a small extent, sodium- and magnesium-containing compounds were improbable. Therefore, the presence of compounds such as $Na_5H_4(PO_4)_3$ (JCPDS card n. 43–54) and β-$NaCaPO_4$ (a buchwaldite phase; JCPDS card n. 29–1193), which could be compatible with some of the detected peaks, had to be excluded.

If the substitution of PO_4^{3-} by CO_3^{2-} ions, typical of a B-type carbonate-apatite, had been dominant, an increase in the Ca/P molar ratio would have been observed [59]. It can be hypothesised that the deposits maintain their apatitic structure thanks to a complex series of substitutions which involve a certain number of groups (e.g., H_2O, CO_3^{2-}, etc.). These species are able to compensate local crystallographic lattice distortions produced by the presence of foreign groups (such as HPO_4^{2-}, which can compensate calcium deficiency) or by anionic and/or cationic vacancies; the latter appear more probable and necessary to keep the overall electroneutrality of the lattice.

On the basis of the relative intensities of the XRD peaks corresponding to the AP40 samples, the only compatible compound found in JCPDS cards was $Ca_{10}(PO_4)_5CO_3F_{1.5}(OH)_{0.5}$. However, since no trace of F^- was detected by EDX on the surface of AP40 samples, the presence of fluorinated apatites (if any) was theoretically possible only for RKKP glasses. For these samples, it could be hypothesised that some F^- ions substituted the hydroxyl groups. Actually, no specific aggregates of fluoroapatite were detected; therefore, it must be hypothesised that F^- ions randomly distributed in the crystallographic lattice of a complex apatitic compound, so contributing to its stabilisation. However, it must be stressed that the I/I_0 values are not completely reliable since the mechanism of micro-crystal deposition may involve effects of preferential displacement.

The presence of HPO_4^{2-} ions was deductible independently of IR spectroscopy, e.g., by utilising the data of the EDX micro-analysis (Table VI). It can be hypothesised that the formed layer was composed of x moles of $Ca_5(PO_4)_3OH$, y moles of $CaHPO_4$, and z moles of $CaCO_3$ combined in an apatitic lattice solid solution with $Ca_{5x+y+z}[(PO_4)_{3x}(HPO_4)_y(CO_3)_z](OH)_x$ stoichiometric formula. By simple stoichiometric calculations on linear systems[1] utilising the data of Tables V and VI, it can be seen that, at increasing immersion times, both glassy systems underwent

notable changes in x, y and z values; the x value increased by about 2.4 times, in apparent compensation for the z increase from about 3 to about 4 moles.

However, it must be observed that the EDX data were affected by an error of about ±6%; consequently, the values obtained by computing elaborations are only indicative, although they provide information on the compositional tendency of the layers formed on the two glasses.

It must be stressed that the IR spectra were not in disagreement with the proposed formula, even if they did not show the bands characteristic of hydroxyl groups. This result has been explained by various authors. De Maeyer *et al.* [60], Nelson and Featherstone [32] observed that, in carbonate-apatites, νOH and δOH modes decreased in intensity at increasing carbonate content. De Maeyer *et al.* [60], Nordstrome and Karlsson [59], Bonel *et al.* [61] explained this trend considering that OH sites were occupied by water molecules.

5. Conclusions

Both glasses, when in contact with a biological fluid, hid their surface under a mimetic calcium-deficient apatite layer. Our investigations disclosed some slight but notable differences between the deposited layers:

(1) even if both the deposits were found to be composed of a calcium deficient carbonate-apatite, the layer formed on the RKKP glass was found to be more calcium deficient;

(2) the presence of the HPO_4^{2-} ion is more evident on RKKP samples;

(3) the layer deposited on the RKKP samples is thinner than on the AP40 ones: this would suggest a slower activity of RKKP with respect to AP40;

(4) the presence of some F^- ions was observed only in the layers formed on the RKKP samples.

These results indicate that the interaction mechanism between glass and surrounding chemical environment is a bit different for the two glassy systems. The differences disclosed, although slight, can account, partially at least, for the different *in vivo* behaviour displayed by AP40 and RKKP glasses. In particular, the most relevant difference could be the presence of F^- ions observed only in the layers formed on the RKKP samples. At this purpose, it is well known that fluorine ions stabilise the apatitic lattice [62, 63] and in low amount have a stimulating effect towards bone reconstruction (very small quantities of F^- ions enhance osteoblast proliferation) [64].

Note

1. The stoichiometric equation $x\mathrm{Ca_5(PO_4)_3OH}\cdot y\,\mathrm{CaHPO_4}\cdot z\mathrm{CaCO_3}$ can be solved for the x, y and z variables by the following linear system:

$$\begin{cases} 5x + y + z = Q_{\mathrm{Ca}} & \text{(moles of } Ca^{2+} \text{ detected)} \\ 3x + y = Q_{\mathrm{P}} & \text{(moles of } P^{5+}\text{, or } PO_4^{3-}\text{, detected)} \\ z = Q_C & \text{(moles of } C^{4+}\text{, or } CO_3^{2-}\text{, detected)} \end{cases}$$

The solutions of this system are:

$$x = 1/2(Q_{\mathrm{Ca}} - Q_{\mathrm{C}} - Q_{\mathrm{P}})$$
$$y = 1/2[5Q_{\mathrm{P}} + 3(Q_{\mathrm{C}} - Q_{\mathrm{Ca}})]$$
$$z = Q_{\mathrm{C}}$$

Acknowledgements

This work was supported by 60% grants from MIUR, Italy.

References

1. L. L. HENCH, *J. Amer. Ceram. Soc.* **74** (1991) 1487.
2. T. KOKUBO, in "Handbook of Bioactive Ceramics," edited by T. Yamamuro, L. L. Hench and J. Wilson (CRC Press, Boca Raton, Florida, 1990), Vol. 1, p. 41.
3. L. L. HENCH, R. J. SPLINTER, W. C. ALLEN and T. K. GREENLEE, *J. Biomed. Mater. Res.* **2** (1971) 117.
4. A. KRAJEWSKI and A. RAVAGLIOLI, *Biomaterials* **9** (1988) 449.
5. A. KRAJEWSKI, A. RAVAGLIOLI, A. BERTOLUZZA, P. MONTI, M. A. BATTAGLIA, A. PIZZOFERRATO, R. OLMI and A. MORONI, *Biomaterials* **9** (1988) 528.
6. A. M. GATTI, D. ZAFFE, G. P. POLI, A. RAVAGLIOLI and A. KRAJEWSKI, in "Clinical Implant Materials. Advances in Biomaterials," edited by G. Heimke, U. Soltéz and A. J. C. Lee (Elsevier Science Publ., Amsterdam, 1990), Vol. 9, p. 579.
7. P. TORRICELLI, M. FINI, G. GIAVARESI, A. KRAJEWSKI, A. RAVAGLIOLI, P. DI DENIA, G. CALIGIURI, M. MATTIOLI-BELMONTE, A. DE BENEDITTIS, G. BIAGINI and R. GIARDINO, in Proc. 5th Meeting and Seminar on Ceramics, Cells and Tissues, Faenza, Ravenna, Italy, 1999, edited by A. Ravaglioli and A. Krajewski (IRTEC-CNR, 1999) p. 205.
8. P. MENGUCCI, A. DI CRISTOFORO, A. DE BENEDITTIS, G. MAJNI, A. KRAJEWSKI, A. RAVAGLIOLI and M. MAZZOCCHI, in Proc. 12th International Symposium on Ceramics in Medicine, Nara, Japan, 1999 (Bioceramics, Vol. 12), edited by H. Ohgushi, G. W. Hastings and T. Yoshikawa (World Scientific Publishing Co. Pte. Ltd., 1999) p. 507.
9. A. TINTI, P. TADDEI, C. B. AZZONI, D. DI MARTINO, A. KRAJEWSKI, M. MAZZOCCHI and A. RAVAGLIOLI, in Proc. 6th Meeting and Seminar on Ceramics, Cells and Tissues, Faenza, Ravenna, Italy, 2000, edited by A. Ravaglioli and A. Krajewski (IRTEC-CNR, 2000) p. 60.
10. A. RAVAGLIOLI and A. KRAJEWSKI, in Proc. 2nd Meeting and Seminar on Ceramics, Cells and Tissues, Faenza, Ravenna, Italy, 1996, edited by A. Ravaglioli and A. Krajewski (IRTEC-CNR, 1996) p. 113.
11. M. FERRARIS, E. VERNÉ, A. RAVAGLIOLI, A. KRAJEWSKI, L. PARACCHINI, J. VOGEL, G. CARL and C. JANA, in Proc. 10th International Symposium on Ceramics in Medicine, Amsterdam, 1997 (Bioceramics, Vol. 10), edited by L. Sedel and C. Rey (Elsevier Science Ltd., Amsterdam, 1997) p. 195.
12. M. KIRSCH, A. KRAJEWSKI, A. RAVAGLIOLI and H. NIESWAND, in Proc. 3rd Meeting and Seminar on Ceramics, Cells and Tissues, Faenza, Ravenna, Italy, 1997, edited by A. Ravaglioli and A. Krajewski (IRTEC-CNR, 1997) p. 9.
13. A. KRAJEWSKI, R. MALAVOLTI and A. PIANCASTELLI, *Biomaterials* **17** (1996) 53.
14. D. ZAFFE, A. KRAJEWSKI, A. RAVAGLIOLI and S. CONTOLI, *J. Mater. Sci. Mater. Med.* **4** (1993) 169.
15. M. MATTIOLI-BELMONTE, A. DE BENEDITTIS, R. A. MUZZARELLI, P. MENGUCCI, G. BIAGINI, M. G. GANDOLFI, C. ZUCCHINI, A. KRAJEWSKI, A. RAVAGLIOLI, E. RONCARI, M. FINI and R. GIARDINO, *ibid.* **9** (1998) 485.

16. G. BIAGINI, R. SOLMI, M. G. GANDOLFI, R. GIARDINO, M. FINI, A. KRAJEWSKI, A. RAVAGLIOLI, P. MENGUCCI, M. MATTIOLI-BELMONTE and R. A. MUZZARELLI, in Proc. 3rd Meeting and Seminar on Ceramics, Cells and Tissues, Faenza (Ravenna, Italy), 1997, edited by A. Ravaglioli and A. Krajewski (IRTEC-CNR, 1997) p. 195.
17. M. G. GANDOLFI, M. FINI, G. BIAGINI, R. GIARDINO, A. KRAJEWSKI, A. RAVAGLIOLI, G. SBARGI, L. SIMONELLI and N. NICOLI-ALDINI, in Proc. 4th European Ceramic Society Conference, Faenza, Ravenna, Italy, 1995 (Bioceramics, Vol. 8), edited by A. Ravaglioli and A. Krajewski (Faenza Editrice, 1995) p. 355.
18. M. FINI, N. NICOLI-ALDINI, M. G. GANDOLFI, M. MATTIOLI-BELMONTE, G. GIAVARESI, C. ZUCCHINI, A. DE BENEDITTIS, S. AMATI, A. RAVAGLIOLI, A. KRAJEWSKI, M. ROCCA, G. A. GUZZARDELLA, G. BIAGINI and R. GIARDINO, *Int. J. Artif. Org.* **20** (1997) 291.
19. A. KRAJEWSKI, A. RAVAGLIOLI, M. MAZZOCCHI, C. B. AZZONI, D. DI MARTINO and P. CARRETTA, in Proc. 5th Meeting and Seminar on Ceramics, Cells and Tissues, Faenza, Ravenna, Italy, 1999, edited by A. Ravaglioli and A. Krajewski (IRTEC-CNR, 1999) p. 111.
20. C. B. AZZONI, P. CARRETTA, D. DI MARTINO, E. R. MOGNASCHI, A. TINTI, P. TADDEI, A. KRAJEWSKI, M. MAZZOCCHI and A. RAVAGLIOLI, in Proc. 7th Meeting and Seminar on Ceramics, Cells and Tissues, Faenza, Ravenna, Italy, 2001, edited by A. Ravaglioli and A. Krajewski (IRTEC-CNR, 2001) p. 230.
21. M. BOSETTI, E. VERNÈ, M. FERRARIS, A. RAVAGLIOLI and M. CANNAS, *Biomaterials* **22** (2001) 987.
22. A. ROSENGREN, S. OSCARSSON, M. MAZZOCCHI, A. KRAJEWSKI and A. RAVAGLIOLI, *ibid.* **24** (2003) 147.
23. P. DUCHEYNE and Q. QIU, *ibid.* **20** (1999) 2287.
24. A. EL GHANNAM, P. DUCHEYNE and I. M. SHAPIRO, *J. Orthop. Res.* **17** (1999) 340.
25. A. P. SERRO, A. C. FERNANDES, B. SARAMAGO and M. H. V. FERNANDES, *J. Biomed. Mater. Res.* **61** (2002) 99.
26. J. LIMA, S. R. SOUSA, A. FERREIRA and M. A. BARBOSA, *ibid.* **55** (2001) 45.
27. A. P. SERRO, A. C. FERNANDES, B. SARAMAGO, J. LIMA and M. A. BARBOSA, *Biomaterials* **18** (1997) 963.
28. J. D. B. FEATHERSTONE, S. PEARSON and R. Z. LE GEROS, *Caries Res.* **18** (1984) 63.
29. "Handbook of X-rays," edited by E. F. Kaelbe (McGraw-Hill, New York, 1967) p. 3.
30. I. IZQUIERDO-BARBA, A. J. SALINAS and M. VALLET-REGÌ, *J. Biomed. Mater. Res.* **47** (1999) 243.
31. K. C. BLAKESLEE and R. A.CONDRATE, *J. Am. Chem. Soc.* **54** (1971) 559.
32. D. G. A. NELSON and J. D. B. FEATHERSTONE, *Calcif. Tissue Int.* **34** (1982) S69.
33. R. J. BELL and P. DEAN, *Discuss. Farad. Soc.* **50** (1970) 55.
34. P. H. GASKELL, *ibid.* **50** (1970) 82.
35. F. S. CASCIANI and R. A. CONDRATE, in Proceedings of the 2nd International Congress on Phosphorous Compounds, Paris, 1980, edited by C. Ean (Phosphorous Publications, 1980) p. 175.
36. A. J. SALINAS, A. I. MARTIN and M. VALLET-REGÌ, *J. Biomed. Mater. Res.* **61** (2002) 524.
37. G. BONEL, *Ann. Chim.* **7** (1972) 127.
38. F. APFELBAUM, H. DIAB, I. MAYER and J. D. B. FEATHERSTONE, *J. Inorg. Biochem.* **45** (1992) 277.
39. D. VIRGO, B. O. MYSEN and I. KUSHIRO, *Science* **208** (1980) 1371.
40. Y. TSUNAWAKI, N. IWAMOTO, T. HATTORI and A. MITSUISHI, *J. Non-Cryst. Solids* **44** (1981) 369.
41. N. J. CLAYDEN, S. ESPOSITO, U. A. JAYASOORIYA, J. SPRUNT and P. PERNICE, *ibid.* **224** (1998) 50.
42. J. ETCHEPARE, *Spectrochim. Acta* **26A** (1970) 2147.
43. *Idem., J. Chem. Phys. Physico-Chem. Biol.* **67** (1970) 890.
44. C. Y. KIM, A. E. CLARK and L. L. HENCH, *J. Non-Cryst. Solids* **113** (1989) 195.
45. C. OHTSUKI, T. KOKUBO and T. YAMAMURO, *ibid.* **143** (1992) 84.
46. M. M. PEREIRA, A. E. CLARK and L. L. HENCH, *J. Biomed. Mater. Res.* **28** (1994) 693.
47. I. REHMAN, L. L. HENCH, W. BONFIELD and R. SMITH, *Biomaterials* **15** (1994) 865.
48. O. P. FILHO, G. P. LA TORRE and L. L. HENCH, *J. Biomed. Mater. Res.* **30** (1996) 509.
49. M. CATAURO, G. LAUDISIO, A. COSTANTINI, R. FRESA and F. BRANDA, *J. Sol-Gel Sci. Technol.* **10** (1997) 231.
50. I. REHMAN, J. C. KNOWLES and W. BONFIELD, *J. Biomed. Mater. Res.* **41** (1998) 162.
51. M. VALLET-REGÌ, I. IZQUIEDO-BARBA and A. J. SALINAS, *ibid.* **46** (1999) 560.
52. H. H. LU, S. R. POLLACH and P. DUCHEYNE, *ibid.* **51** (2000) 80.
53. S. RADIN, P. DUCHEYNE, S. FALAIZE and A. HAMMOND, *ibid.* **49** (2000) 264.
54. I. REHMAN, M. KARSH, L. L. HENCH and W. BONFIELD, *ibid.* **50** (2000) 97.
55. P. SEPULVEDA, J. R. JONES and L. L. HENCH, *ibid.* **61** (2002) 301.
56. J. R. JONES, P. SEPULVEDA and L. L. HENCH, *J. Biomed. Mater. Res. (Appl. Biomater.)* **58** (2001) 720.
57. M. FINI, G. GIAVARESI, N. NICOLI ALDINI, P. TORRICELLI, G. MORRONE, G. A. GUZZARDELLA, R. GIARDINO, A. KRAJEWSKI, A. RAVAGLIOLI, M. MATTIOLI BELMONTE, A. DE BENEDITTIS and G. BIAGINI, *J. Mater. Sci. Mater. Med.* **11** (2000) 579.
58. C. LOTY, J. M. SAUTIER, H. BUOLEKBACHE, T. KOKUBO, H. M. KIM and N. FOREST, *J. Biomed. Mater. Res.* **49** (2000) 423.
59. E. G. NORDSTROME and K. H. KARLSSON, *J. Mater. Sci. Mater. Med.* **1** (1990) 182.
60. E. A. P. DE MAEYER, R. M. H. VERBEECK and D. NAESSEN, *Inorg. Chem.* **32** (1993) 5709.
61. G. BONEL, J. C. LABARTHE and C. VIGNOLES, in "Physicochimie et Cristallographie des apatites d'interest biologiques" (CNRS, Paris, 1975) p. 117.
62. K. SUNDARSANAN, R. A. YOUNG and A. S. POSNER, *Nature* **204** (1964) 1050.
63. M. L. HAIR, in "The chemistry of Biosurfaces," (Marcel Dekker, New York, 1972), Vol. 2, p. 699.
64. K. H. LAU and D. J. BAYLINK, *J. Bone Miner. Res.* **13** (1998) 1660.

Received 5 November 2003
and accepted 20 July 2004